Published in final edited form as:
J Immunol. 2009 April 1; 182(7): 4226–4236. doi:10.4049/jimmunol.0800771.

B Cell Proliferation, Somatic Hypermutation, Class Switch Recombination, and Autoantibody Production in Ectopic Lymphoid Tissue in Murine Lupus

Dina C. Nacionales[1,*], **Jason S. Weinstein**[1,*], **Xiao-Jie Yan**[2], **Emilia Albesiano**[2], **Pui Y. Lee**[1], **Kindra M. Kelly-Scumpia**[1], **Robert Lyons**[1], **Minoru Satoh**[1], **Nicholas Chiorazzi**[2], and **Westley H. Reeves**[1,†]

[1]Division of Rheumatology & Clinical Immunology and Center for Autoimmune Disease, University of Florida, Gainesville, FL 32610-0221

[2]The Feinstein Institute for Medical Research, North Shore-Long Island Jewish Health System, Manhasset, NY 11030

Abstract

Intraperitoneal exposure of non-autoimmune mice to tetramethylpentadecane (TMPD) causes lupus and the formation of ectopic lymphoid tissue. Although associated with humoral autoimmunity, it is not known whether antibody responses develop within ectopic lymphoid tissue or if B cells only secondarily migrate there. We show that ectopic lymphoid tissue induced by TMPD not only resembles secondary lymphoid tissue morphologically, but also displays characteristics of germinal center reactions. Proliferating T and B lymphocytes were found within ectopic lymphoid tissue, activation-induced cytidine deaminase was expressed, and class switched B cells were present. The presence of circular DNA intermediates, a hallmark of active class switch recombination, suggested that class switching occurs within the ectopic lymphoid tissue. Individual collections of ectopic lymphoid tissue ("lipogranulomas") from the same mouse contained different B cell repertoires, consistent with local germinal center-like reactions. Class-switched anti-RNP autoantibody producing cells were also found in the lipogranulomas. Somatic hypermutation in the lipogranulomas was T cell dependent, as was the production of isotype-switched anti-Sm/RNP autoantibodies. Thus, ectopic lymphoid tissue induced by TMPD recapitulates many of the functional characteristics of secondary lymphoid tissue and contains autoantibody secreting cells, which may escape from normal censoring mechanisms in this location.

Keywords

B cells; T cells; ectopic lymphoid tissue; tetramethylpentadecane; germinal center

INTRODUCTION

Secondary lymphoid tissue, which includes lymph nodes, mucosal-associated lymphoid tissues, and the spleen, is organized to concentrate foreign antigens, placing the cells responsible for mounting an antigen-specific immune response to these antigens (T and B lymphocytes and dendritic cells) in close proximity (1, 2). The tissue is organized into

[†]Correspondence to: Westley H. Reeves, Division of Rheumatology & Clinical Immunology, University of Florida, PO Box 100221, Gainesville, FL 32610-0221, Phone: 352-392-8600; Fax: 352-846-1858, whreeves@ufl.edu.
[*]DC Nacionales and JS Weinstein contributed equally to this work

discrete zones containing T cells and dendritic cells (the periarteriolar lymphoid sheath) and B cells and follicular dendritic cells (the primary follicles). The chemokines CCL19 (ELC) and CCL21 (SLC), which attract T lymphocytes and dendritic cells, and CXCL13 (BLC), which attracts B lymphocytes, play an important role in establishing the compartmentalization of secondary lymphoid tissues into discrete T and B cell zones (3). Antigen-specific B cells appear initially at the periphery of the periarteriolar lymphoid sheath forming primary foci, which are sites of interclonal competition for antigen among unmutated B cells (4). Subsequently, these give rise to a second responding population in the follicle, germinal center B cells. Germinal centers are sites of intraclonal competition for antigen and survival signals between mutated sister lymphocytes (4). The germinal center reaction regulates antigen-specific clonal evolution during the development of B cell memory (5). It is characterized by somatic hypermutation (SHM) of immunoglobulin complementarity determining regions (CDRs), class switch recombination (CSR), clonal expansion (proliferation), and antigen-driven affinity maturation of B cells, expression of activation induced cytidine deaminase (AID), and a requirement for $CD40L^+$ T cells (5). B cells in newly formed germinal centers generally are often oligoclonal, consisting of 1-3 clones (6).

The formation of ectopic (tertiary) lymphoid tissue in response to inflammation has been termed “lymphoid neogenesis” because it recapitulates many aspects of secondary lymphoid tissue development (1, 7). Like secondary lymphoid tissue, the organization of ectopic lymphoid tissue is dependent on CCL19 (ELC), CCL21 (SLC), and CXCL13 (BLC) (1). Interestingly, lymphoid neogenesis is strongly associated with autoimmunity and the formation of autoantibodies (8). Autoimmune disorders associated with the formation of ectopic lymphoid tissue include Hashimoto’s thyroiditis, Sjogren’s syndrome, rheumatoid arthritis, and myasthenia gravis (1). We have shown that the intraperitoneal injection of the hydrocarbon pristane (2, 6, 10, 14 tetramethylpentadecane, TMPD) gives rise to the formation of ectopic lymphoid tissue and a chronic immune reaction culminating in the development of lupus (9). In contrast, other hydrocarbon oils, such as medicinal mineral oil, induce the formation of ectopic lymphoid tissue but not lupus (10). Inflammatory tissue generated in response to TMPD consists of dendritic cells, monocytes, T cells, and B cells, often organized into discrete zones reminiscent of lymph node architecture, which is vascularized by $MECA\text{-}79^+$ high endothelial venules (9). The ectopic lymphoid tissue is organized into discrete nodular “lipogranulomas” (11). CCL19, CCL21, and CXCL13 all are expressed in the lipogranulomas and likely play a role in recruiting immune cells into them (9).

In this study we show that the lipogranulomas not only morphologically resemble lymphoid organs but also display some of the characteristics of germinal center reactions, namely proliferation of T and B lymphocytes, T cell dependent SHM of immunoglobulin variable regions, expression of AID, and CSR. IgG1 and IgG2a hypergammaglobulinemia induced by TMPD as well as the production of isotype-switched autoantibodies required the presence of T cells. Moreover, autoantibody secreting cells were present in the lipogranulomas, consistent with the possibility that they can be generated within the ectopic (tertiary) lymphoid tissue.

MATERIALS AND METHODS

Mice

Four-week-old female BALB/cJ mice were purchased from Jackson Laboratory (Bar Harbor, ME) and housed in barrier cages. At 3 months of age, they received a single intraperitoneal (i.p.) injection (0.5 ml) of either TMPD (Sigma-Aldrich, St. Louis, MO) or medicinal mineral oil (Harris Teeter, Mathews, NC). Peritoneal cells, lipogranulomas, and

blood were harvested 12-20 weeks later. In some experiments female T cell receptor deficient (B6.129P2-*Tcrb*^{tm1Mom}*Tcrd*^{Tm1Mom}, backcross generation N12) and C57BL/6J mice (Jackson) were used. These studies were approved by the Institutional Animal Care and Use Committee.

Immunohistochemistry and immunofluorescence

Lipogranulomas were excised from the peritoneal wall after peritoneal lavage, fixed with 4% paraformaldehyde, and embedded in paraffin. Immunohistochemistry was carried out by the Molecular Pathology and Immunology Core at University of Florida using the DAKO Autostainer protocol. Briefly, 4 μm serial sections were de-paraffinized and then blocked with Sniper (Biocare Medical, Walnut Creek, CA). Sections were incubated with rat anti-mouse CD45R (B220) (BD Biosciences, San Jose, CA), CD3 (Serotec, Raleigh, NC), or Ki-67 (Dako Cytomation, Carpinteria, CA) for 1 hour followed by incubation with non-biotinylated rabbit anti-rat immunoglobulin antibodies (Vector, Burlingame, CA) for 30 minutes. Staining was visualized using Mach Gt x Rb HRP polymer (Biocare Medical, Walnut Creek, CA), the chromagen Cardassian DAB (Biocare Medical, Walnut Creek, CA) and Mayer's hematoxylin counterstain. Tissue sections also were stained with antibodies against follicular dendritic cells (FDC-M1, BD Biosciences) and processed for immunohistochemistry as above.

To detect IgM and IgG in the lipogranulomas, de-paraffinized sections were stained with either FITC-conjugated goat anti-mouse IgG or IgM (Southern Biotechnology, Birmingham, AL), mounted using Vectashield mounting medium with DAPI (Vector) and examined by fluorescence microscopy.

Bromodeoxyuridine (BrdU) labeling of B and T cells

BrdU was administered to BALB/cJ mice (0.2 mg BrdU i.p. every 4 hours for 3 doses) and again one day before euthanasia. Peritoneal lipogranulomas from each mouse were excised and pooled. Single cell suspensions were made by collagenase treatment (9). Spleen cells were also prepared using collagenase treatment. The isolated cells were incubated with APC-conjugated anti-BrdU antibodies, plus anti-CD3-FITC and anti-CD19-PE antibodies (BD Biosciences) and analyzed by flow cytometry. Appropriate isotype controls were used to evaluate background fluorescence. Isolated lipogranuloma cells were washed in staining buffer (PBS supplemented with 0.1% NaN_3 and 1% bovine serum albumin) and pre-incubated for 20 minutes with 1 μg of anti-CD16 (BD Biosciences) and 0.5 μl rat serum (Sigma Aldrich) at 4°C in 20 μl of staining buffer to block Fc binding. Primary antibodies were then added at pre-titrated amounts and incubated for 20 minutes at 4°C, followed by washing in staining buffer. Intracellular BrdU labeling was performed after permeabilization with BD Cytoperm plus using the APC BrdU flow kit following the manufacturer's instructions (BD Biosciences). After gating on $B220^+$ or $CD4^+$ lymphocytes, the percentage of $BrdU^+$ cells was determined by flow cytometry as above. Data were acquired on a CyAn ADP flow cytometer (Dako, Fort Collins, Colorado) and analyzed with FCS Express Version 3 (DeNovo Software, Thornhill, Ontario, Canada). At least 50,000 events per sample were acquired and analyzed using size gating to exclude dead cells.

Ki-67 staining of B and T cells

Single-cell suspensions were made from lipogranulomas and spleen, and proliferating cells were surface-stained with anti-B220 and anti-CD4, followed by permeabilization with cold 70% ethanol at −20° for 3 hours. Cells were then analyzed for intracellular staining with anti-Ki-67 antibodies (BD Biosciences) using the manufacturer's protocol. After gating on $B220^+$ or $CD4^+$ lymphocytes, the percentage of Ki-67^+ cells was determined by flow cytometry as above.

RT-PCR analysis of AID and class switched H-chain transcripts

Total RNA from individual lipogranulomas excised from TMPD- or mineral oil-treated mice was isolated using Trizol (Invitrogen Life Technologies, Carlsbad, California) and precipitated with isopropanol. The pellets were washed with cold 75% (v/v) ethanol and resuspended in diethyl pyrocarbonate (DEPC)-treated water. One μg of RNA was treated with DNase I (Invitrogen) to remove genomic DNA and reverse transcribed to cDNA using Superscript First-Strand Synthesis System for RT-PCR (Invitrogen). Conventional PCR amplification was carried out in a PTC-100 Programmable Thermal Controller (MJ Research, Inc., Waltham, MA) using primers for AID (forward- GAG GGA GTC AAG AAA GTC ACG CTG GA ; reverse- GGC TGA GGT TAG GGT TCC ATC TCA) and β-actin (12). Real-time PCR was performed using SYBR Green core reagents (Applied Biosystems, Foster City, CA) and a DNA Engine Opticon 2 continuous fluorescence detector (MJ Research). PCR primers were as follows: AID forward-CCT CCT GCT CAC TGG ACT CC; AID reverse-AGG CTG AGG TTA GGG TTC CA; 18S forward-AGG CTA CCA CAT CCA AGG AA; 18S reverse-GCT GGA ATT ACC GCG GCT. AID expression was normalized to the expression of an endogenous control (18s RNA) using the comparative ($2^{-\Delta\Delta Ct}$) method (1). Data are expressed relative to the sample with the lowest expression level. For detecting IgM and IgG1 transcripts, a mixture of 8 consensus forward primers (VHF1-8) and isotype specific Cμ and Cγ1 reverse primers were used (13). Primers were synthesized by Invitrogen. PCR products were analyzed on 1% agarose gels and stained with ethidium bromide.

CSR assay

The occurrence of active CSR in ectopic lymphoid tissue (TMPD or mineral oil induced "lipogranulomas") was evaluated by detecting looped out circular DNAs as described (14). Briefly, total RNA was isolated from individual lipogranulomas and treated with DNase I as above, and "circle transcripts" were amplified as follows: initial denaturation 95°C for 9 min followed by 35 cycles of PCR (94°C for 30 sec, 58°C for 60 sec) using 0.025 U of Taq DNA polymerase (Invitrogen), 2.0 mM $MgCl_2$, and 1 μM each of isotype-specific I-region primers (Iγ1F or Iγ2aF) and a Cμ reverse primer (14). PCR products were separated on a 1% agarose gel and stained with ethidium bromide.

Immunoglobulin V-D-J sequence analysis

To determine VDJ gene usage, 1 μl cDNA was amplified using pooled forward (VHF1-8) and reverse (VHR2) primers (Fig. 3A) (13). The reaction was carried out in a 20 μl volume using 1.25 nM pooled VHF and 2.5 nM VHR2 primers containing 1X PCR buffer, 1.5 mM $MgCl_2$, 200 μM dNTPs, and 0.05 U of Taq DNA polymerase (Invitrogen), in a PTC-100 Programmable Thermal Controller (MJ Research) as follows: denaturation at 94°C for 30 sec, annealing at 52°C for 30 sec, and extension at 72°C for 1 min. After 30 cycles, extension was continued at 72°C for an additional 10 min. The PCR product was cloned into a TA vector (pCR4, Invitrogen) and sequenced using an Applied Biosystems Model 373 Stretch DNA Sequencer, 377 DNA Sequencer, or 3100 Genetic Analyzer using a T7 sequencing primer. The determined sequences were verified by sequencing in the reverse direction using a T3 sequencing primer. V_H, D, and J_H sequences were identified by searching the Ig-BLAST and IMGT/V-Quest databases using MacVector software (Accelrys Inc., San Diego, CA).

ELISA

Anti-nRNP/Sm antigen-capture ELISAs were performed as described (15). Antigen-coated wells were incubated with 100 μl mouse sera diluted 1:500 in blocking buffer for 1 hr at 22°C, washed three times with TBS/Tween 20, and incubated with 100 μl alkaline

phosphatase-labeled goat anti-mouse IgG or IgM (1:1000 dilution) for 1 hr at 22°C. After washing, the plates were developed with *p*-nitrophenyl phosphate substrate (Sigma). Optical density at 405 nm (OD_{405}) was read using a VERSAmax microplate reader (Molecular Devices Corporation, Sunnyvale, CA). Standard curves were generated using serial dilutions of a murine anti-U1-70K monoclonal antibody (2.73). Concentrations of anti-Sm/RNP autoantibodies were calculated using a four-parameter logistic equation as part of the Softmax Pro 3.0 ELISA plate reader software. Total levels of IgG1, IgG2a, IgG3, and IgM were measured by ELISA as described (16).

Quantification of plasmablasts

Single-cell suspensions were made using spleen and lipogranuloma tissue from five TMPD-treated BALB/c mice. Cells were stained with APC-conjugated anti-B220 and PE-conjugated anti-CD138 antibodies (BD Pharmingen) and analyzed by flow cytometry as above.

ELISPOT assay for total immunoglobulin

Lipogranulomas and splenocytes from TMPD treated mice were harvested, analyzed by flow cytometry to determine B cell numbers (anti-CD19), and plated (3×10^5 cells/well) in quadruplicate on Multiscreen HTS plates (Millipore, Billerica, MA) coated with rat IgG anti-mouse light chain antibodies (κ and λ chain specific, 3 μg/ml each, from BD Pharmingen). The cells were incubated overnight before adding a combination of alkaline phosphatase-conjugated rat anti-mouse IgG1, IgG2a, IgG2b antibodies (1:1000 dilution). Spots were developed overnight with BCIP/NBT (Pierce Chemical Co., Rockford, IL). The number of antibody secreting lipogranuloma cells and splenocytes per 100,000 B cells was determined by counting the spots using a dissecting microscope.

ELISPOT assay for anti-RNP autoantibodies

The production of anti-U1A (a subset of anti-RNP) autoantibodies in the ectopic lymphoid tissue also was examined by ELISPOT assay. A human full-length U1A cDNA was obtained by RT-PCR (PTC-100 Programmable Thermal Controller (MJ Research, Inc., Waltham, MA) from normal human PBMC cDNA. The forward primer was GCG GAT CCG CAG TTC CCG AGA CCC GCC CTA ACC AC Bam HI and reverse primer was GCA AGC TTC TAC TTC TTG GCA AAG GAG ATG TTC Hind III. The amplified fragment was inserted between the BamHI and HindIII sites of pET28A (Invitrogen) in-frame with the 6His sequence. The vector was used to transform *E. coli* BL21 DE3 and recombinant protein was expressed by growing in LB medium containing 10 μg/ml kanamycin and 2 mM IPTG. Four hours later, the bacteria were lysed using 6 M guanidine HCl + 0.5 mM phenylmethylsulfonyl fluoride and 0.3 TIU/ml aprotinin. Recombinant protein was purified using Ni-NTA resin columns (Sigma). The protein was eluted with 6 M urea.

Reactivity with serum anti-RNP autoantibodies from TMPD-treated mice was verified by ELISA. The microtiter plate wells (Immobolizer Amino; Nunc, Napeville, IL) were coated with 1 μg/ml purified recombinant antigen in BBS overnight at 5° C. The remainder of the ELISA was carried out as described above. Sera from 20 anti-Sm/RNP positive TMPD-treated mice and 20 untreated controls were tested at a 1:500 dilution followed by 1:1000 alkaline phosphatase-conjugated goat anti-mouse immunoglobulin antibodies (Southern Biotechnology). Using the SoftMax Pro 3.0 software, OD_{405} values were converted to units with a standard curve based on a serially diluted prototype serum.

For the ELISPOT assays, lipogranuloma cells from TMPD treated BALB/cJ mice were harvested and plated on Multiscreen HTS plates (Millipore) coated overnight at 4°C with

either recombinant U1A protein (5 μg/ml) *or BSA* followed by alkaline phosphatase-conjugated goat anti-mouse IgG or IgM antibodies (1:1000 dilution, Southern Biotechnology). Spots were developed overnight with BCIP/NBT (Pierce) and counted as above.

RESULTS

Lipogranulomas developing in the peritoneum of TMPD- or mineral oil-treated mice are a form of ectopic lymphoid tissue (9). We investigated whether these structures also exhibit functional characteristics consistent with germinal center reactions, such as SHM, CSR, and antigen-driven, T cell-dependent proliferation of B lymphocytes.

Lymphocyte proliferation in TMPD-induced ectopic lymphoid tissue

As shown previously (9), serial sections of lipogranulomas from TMPD-treated mice revealed contiguous aggregates of $B220^+$ and $CD3^+$ cells (Fig. 1A). Ki-67^+ cells were found in the same region, consistent with the presence of proliferating lymphocytes (Fig. 1A). However, it was difficult to determine from these sections whether T cells, B cells, or both were proliferating. To address this question, pooled lipogranulomas were analyzed by flow cytometry using anti-B220, CD4, and Ki-67 antibodies. A small percentage of $B220^+$ (4.91%) and $CD4^+$ lymphocytes (3.85%) was Ki-67^+ (Fig. 1B). To confirm the presence of proliferating B and T lymphocytes in the ectopic lymphoid tissue, TMPD-treated mice were injected with BrdU (0.2 mg every 4 hours for 3 doses) and euthanized the following day. Incorporation of BrdU by B and T cells in the lipogranulomas and spleen was determined by flow cytometry using anti-BrdU antibodies. $BrdU^+$ B ($B220^+$) and T ($CD3^+$) cells were present in both the lipogranulomas and the spleen (Fig. 1C). There was a significantly higher percentage of $BrdU^+$ B and T cells in the lipogranulomas compared with spleen ($p = 0.028$), indicating that B and T cell proliferation was greater in the ectopic lymphoid tissue than in secondary lymphoid tissue (spleen). Follicular dendritic cells could not be identified in the ectopic lymphoid tissue after staining with FDC-M1 antibodies (Fig. 1A), whereas strong staining of follicular dendritic cells could be demonstrated in the spleen (not shown).

AID expression and CSR in TMPD-induced ectopic lymphoid tissue

As B cell proliferation in lymphoid follicles is linked to SHM and Ig repertoire diversification (17), we examined the expression of AID, a marker of CSR and SHM, in TMPD and mineral oil lipogranulomas. By RT-PCR, expression of AID was demonstrated in both TMPD and mineral oil induced lipogranulomas but not in peritoneal exudate cells (Fig. 2A). However, the expression appeared lower than in the spleen. Quantitative PCR confirmed that AID expression was lower in lipogranulomas than spleen from TMPD-treated mice, whereas the levels were comparable in lipogranulomas vs. spleen of mineral oil treated mice **(**Fig. 2A, **right)**. The expression of AID was higher in TMPD or mineral oil lipogranulomas than in peritoneal exudate cells.

Since AID expression is required for immunoglobulin class switching, we examined whether IgG-producing B cells were present in the ectopic lymphoid tissue. Class switching to IgG1 and IgG2a, which requires T cells and is characteristic of germinal center reactions, was detected using conventional RT-PCR. Variable levels of μ H-chain mRNA could be detected in nearly all lipogranulomas from either TMPD- or mineral oil-treated mice and high levels were also found in the spleen (Fig. 2B). In contrast, γ1 H-chain mRNA was more abundant in the ectopic lymphoid tissue from TMPD-treated mice in comparison with mineral oil treated mice. At least low levels of γ1 H-chain were detectable by RT-PCR in 11/12 TMPD lipogranulomas vs. 1/12 mineral oil lipogranulomas **(**Fig. 2B, **right)**.

CSR is accompanied by the looping out of a DNA segment containing Cμ and other C_H genes generating closed circular DNAs with isotype-specific I-Cμ transcripts. *In vitro*, these "circle transcripts" are completely removed within 48 hours and detection of circle transcripts by PCR is indicative of active CSR (14). We used the presence of circle transcripts to evaluate whether the lipogranulomas were a site of active CSR. Consistent with the data shown in Fig. 2B, γ2a or γ1 (not shown) circle transcripts were detected in some of the TMPD-induced lipogranulomas (3 out of 12 total), but were not detected in mineral oil lipogranulomas (0 out of 11) (Fig. 2C). [increase number of granulomas, circle transcripts occurred rarely in mineral oil granulomas, as well] As a further confirmation, lipogranulomas from mineral oil or TMPD-treated mice were stained with FITC-conjugated anti-immunoglobulin antibodies (μ or γ chain specific) and examined by fluorescence microscopy (Fig. 2D). Mineral oil and TMPD lipogranulomas both contained cells expressing μ H-chain, whereas γ H-chain was detected only in TMPD lipogranulomas.

Individual lipogranulomas from a single mouse contain different populations of B cells

Germinal center reactions are characterized by oligoclonal expansions of antigen-specific B cells with somatically mutated immunoglobulin H and L chains. We therefore examined the B cell repertoire in single lipogranulomas (ectopic lymphoid tissue) induced by TMPD or mineral oil treatment. Figure 3A shows the primers used to analyze immunoglobulin V_H gene expression in the ectopic lymphoid tissue. A total of 78 sequences isolated from 7 individual lipogranulomas from three TMPD-treated mice and 22 sequences isolated from 4 individual lipogranulomas from two mineral oil treated mice were analyzed. Figure 3B depicts the distribution of V-D-J segment usage in individual lipogranulomas from three representative mice. Lipogranulomas #137, 139, and 140 were isolated from a single TMPD-treated mouse, lipogranulomas #190 and 193 from another mouse, and lipogranulomas #201 and 204 from a third mouse. Diverse H-chain sequences were obtained from each individual lipogranuloma. In some cases, several identical or closely related sequences were obtained from the same lipogranuloma. For example, six identical, somatically mutated rearrangements comprised of VH36-60-DFL16.1-JH4 were obtained from lipogranuloma #137 and 4 of 7 clones obtained from lipogranuloma #139 used J558.45-DFL16.1-JH1 segments **(Figs.** 3B **and** 4A**)**. One sequence from lipogranuloma #139 and six from lipogranuloma #137 bore a VH36-60-DFL16.1-JH4 rearrangement (Fig. 3B, indicated by *). However, sequence analysis showed that the somatic mutations found in the sequence from lipogranuloma #139 differed substantially from those in lipogranuloma #137, indicating that these sequences were clonally unrelated (Fig. 4A). Four sequences from granuloma #139 and two from #140 did have identical germline J558.45-DFL16.1-JH1 sequences (indicated by †). However, as all sequences were in a germline configuration, it could not be determined whether they were clonally related or derived from two clones that independently rearranged the same V-D-J segments. Sequences from the remaining five granulomas from TMPD-treated mice contained no shared sequences. VH36-60 sequences were isolated frequently from TMPD-, but not mineral oil-induced lipogranulomas (9 out of 78 vs. 0 out of 22 sequences).

The sequences recovered from mineral oil lipogranulomas were also diverse (Fig. 3C). As in the TMPD lipogranulomas, there were occasional examples of the same V-D-J combination being found in more than one lipogranuloma (Fig. 3C, indicated by **). In this case, the sequences were identical (Fig. 4B). However, as was true of the shared sequences in granulomas #139 and 140 (above), the sequences were germline, making it difficult to evaluate whether they were derived from a single clone or two independent clones with the same V-D-J segments.

As suggested by the representative sequences shown in Fig. 4B, the H-chain sequences from ectopic lymphoid tissue in mineral oil treated mice contained fewer somatic mutations than those from TMPD-treated mice. The total somatic mutation frequency in the heavy chain of mice treated with TMPD was 4.9% (607 mutations/12466 bases) in contrast to 0.8% (37 mutations/4336 bases) in mineral oil treated mice. As shown in Table I, the somatic mutations were found predominantly in the CDR regions of sequences obtained from both TMPD- and mineral oil- induced ectopic lymphoid tissue (replacement/silent mutation ratios of 7.2 and 8, respectively, for the CDR regions of TMPD and mineral oil-treated mice vs. 1.7 and 2.0 for the framework regions), suggesting that in both cases, somatic mutations were generated through a process of antigen-selected affinity maturation.

Taken together, these data indicate that the B cells from ectopic lymphoid tissue induced by TMPD or mineral oil in non-immunized mice were clonally diverse, although there was a suggestion that certain clones may predominate within individual lipogranulomas and that VH36-60, an H-chain that is utilized preferentially by B cells with rheumatoid factor or rheumatoid factor-anti-DNA dual reactivity (18, 19), is used considerably more frequently in TMPD-vs. mineral oil-induced ectopic lymphoid tissue. We found little evidence for sharing of B cell clones between individual lipogranulomas, as might be expected if the ectopic lymphoid tissue was populated by B cells arising from another location, such as the spleen or lymph nodes.

SHM in TMPD-treated mice is T cell-dependent

SHM of immunoglobulin genes occurring during the germinal center reaction usually requires $CD40L^+$ T cells (20). However, both inside and outside of germinal centers, SHM sometimes may be T cell-independent (21-23). To investigate the role of T cells in generating the somatic mutations in H-chain sequences from B cells in TMPD-induced ectopic lymphoid tissue, we treated B6.129P2-*Tcrb*^{tmlMom} *Tcrd*^{TmlMom} (T cell receptor β-chain and δ-chain deficient) and wild type C57BL/6J mice with TMPD and analyzed H-chain sequences from the lipogranulomas 3 months later. V-D-J sequences from TcR deficient mice had a very low rate of SHM (1 mutation/3252 total bases, 0.03%), whereas sequences from C57BL/6J mice had a more than 20-fold higher rate (12 mutations/1626 bases, 0.7%). Significantly, these mutations were found mainly in the CDR regions (Table II). The greatly increased number of somatic mutations in wild type vs. TcR deficient mice, clustering of mutations in the CDRs, and the relatively low error rate reported for Taq polymerase (~ 1 error per 10,000 bases) argue that the observed base changes represent true somatic hypermutation and not merely polymerase errors. These data provide further evidence that the SHM seen in ectopic lymphoid tissue from TMPD-treated mice was generated through a germinal center-like reaction.

TMPD-induced hypergammaglobulinemia and autoantibody production are also T cell dependent

Two of the characteristic immune abnormalities induced by TMPD treatment are induction of polyclonal hypergammaglobulinemia and the development of IgM and IgG autoantibodies, such as anti-RNP/Sm, associated with SLE. Since CSR to γ1 and γ2a H-chain occurs in TMPD-induced ectopic lymphoid tissue (Fig. 2C), we investigated whether the increased production of polyclonal serum IgG and IgG autoantibodies requires the presence of T cells. Total immunoglobulin levels were determined (ELISA) in sera from TcR deficient and wild type mice treated with TMPD 3 months earlier. Levels of IgM and IgG3 were comparable in wild type vs. knockout mice (Fig. 5A) consistent with the fact that IgM and IgG3 antibody production is largely T cell independent. However, IgG1 and IgG2a levels were significantly higher in the wild type mice (Mann Whitney $p = 0.008$ and $p =$

0.03, respectively), indicating that the TMPD-induced polyclonal increase in these isotypes was T cell mediated.

To determine whether some of the T cell-dependent immunoglobulin production was derived from B cells present in the lipogranulomas, ELISPOT assays were performed using isolated lipogranuloma cells and splenocytes. As shown in Figure 5B, pooled lipogranuloma B cells from TMPD-treated mice secreted immunoglobulin of T cell dependent isotypes (IgG1, IgG2a, IgG2b) at a frequency similar to that in the spleen. Although the percentage of $B220^{+}CD138^{+}$ plasmablasts was lower in the lipogranulomas compared to spleen (Fig. 5C), the frequency and size of the spots produced by lipogranuloma and splenic B cells was similar suggesting that individual cells from the two locations secreted comparable amounts of polyclonal immunoglobulin. We previously showed that after immunization with exogenous antigen, T cells from the lipogranulomas secrete IL-21, which has been shown to play a role in plasma cell differentiation (24). These data indicate that lipogranuloma cells actively secrete antibodies of T-cell dependent isotypes.

Finally, we examined the role of ectopic lymphoid tissue induced by TMPD in the pathogenesis of lupus-associated autoantibodies against the U1 small ribonucleoprotein (anti-Sm and anti-RNP antibodies). IgM anti-RNP/Sm autoantibodies (ELISA) were detected at low, but comparable, levels in the sera of wild type and TcR knockout mice (Fig. 6A). In contrast, IgG anti-nRNP/Sm autoantibodies were produced by wild type animals but the levels in TcR deficient mice were not statistically different than those in untreated controls (Fig. 6B). These experiments suggested that not only was the induction of polyclonal IgG1 and IgG2a by TMPD T cell dependent (Fig. 5), but also the appearance of class-switched serum autoantibodies required T cells, a characteristic of autoantibodies generated during germinal center reactions.

The presence in ectopic lymphoid tissue of B cells producing class-switched autoantibodies against the U1 small ribonucleoprotein was investigated using an ELISPOT for anti-U1A (anti-RNP) autoantibodies. The purified recombinant U1A antigen used for ELISPOT assays was reactive with sera from 19/20 anti-RNP and/or anti-Sm positive TMPD-treated BALB/c mice, but not with 20 normal mouse sera (Fig. 6C). As shown in Fig. 6D, left panel, large numbers of IgM anti-U1A autoantibody secreting cells were detected in cells obtained from TMPD-induced ectopic lymphoid tissue, but not in ectopic lymphoid tissue induced by medicinal mineral oil, which does not induce serum anti-RNP or anti-Sm autoantibodies. Similarly, IgG anti-U1A autoantibody secreting cells were detected in TMPD-induced ectopic lymphoid tissue, but not in mineral oil-induced ectopic lymphoid tissue (Fig. 6D, right panel). We next compared the frequencies of anti-U1A secreting B cells in the lipogranulomas vs. spleen of mice that were positive for serum anti-RNP autoantibodies (Fig. 6E). A substantial difference in the frequency of anti-U1A secreting B cells in the lipogranulomas vs. the spleen was observed ($p = 0.01$, Mann Whitney test). There also was a significant difference in the frequencies of cells in the lipogranulomas secreting anti-U1A autoantibodies vs. antibodies against a control foreign antigen, bovine serum albumin (BSA) ($p = 0.03$), suggesting that autoantibody producing cells may preferentially localize to or develop within the ectopic lymphoid tissue.

These experiments indicate that class-switched autoantibody producing cells were present within the ectopic lymphoid tissue and were secreting autoantibodies. Taken together, the data in Figures 5 and 6 suggest that the increased polyclonal IgG as well as the IgG anti-RNP autoantibodies in the sera of TMPD-treated mice are likely to be at least partially derived from B cells/plasma cells in the ectopic lymphoid tissue.

DISCUSSION

Structures morphologically and developmentally resembling secondary lymphoid organs (ectopic lymphoid tissue) form at the sites of chronic inflammation, a process known as lymphoid neogenesis (1, 7, 25). There is a strong association of lymphoid neogenesis with humoral autoimmunity (1). However, the role of ectopic lymphoid tissue in initiating immune/autoimmune responses, as opposed to serving as a reservoir for B lymphocytes previously activated elsewhere, has not been fully defined. In NZB/W lupus mice, plasma cells are activated in the spleen and secondarily migrate to inflamed tissues, such as the kidney (26, 27), whereas in patients with rheumatoid arthritis or Sjogren's syndrome ectopic lymphoid tissue may represent a site of antigen-dependent B cell differentiation consistent with a true germinal center reaction (28-30).

Intraperitoneal exposure to TMPD induces lupus in mice (31, 32) with formation of ectopic lymphoid tissue (9), consisting of "lipogranulomas", discrete nodules attached to the mesothelial lining of the peritoneal cavity (11). In certain strains of mice, notably BALB/cAnPt, plasma cell neoplasms develop in the lipogranulomas after several months (33). Closer examination shows that the lipogranulomas morphologically resemble secondary lymphoid tissue, with discrete B cell and T cell-dendritic cell rich zones, MECA-79$^+$ high endothelial venules, and the expression of an array of lymphoid chemokines characteristic of developing lymphoid tissue (9). Following immunization, T cells and B cells specific for exogenous test antigens (NP-KLH and NP-OVA) are enriched in TMPD-lipogranulomas and individual lipogranulomas frequently contain monoclonal populations of proliferating NP-specific B cells along with proliferating carrier specific T cells (24).

The objective of the current study was to see if autoimmune responses can develop within foci of chronic inflammation in lupus. T and B cell proliferation and AID expression as well as SHM and CSR of immunoglobulin genes were found in TMPD-induced lipogranulomas. In addition, we report that B cells actively secreting a prototypical lupus autoantibody, anti-U1A, are enriched in the ectopic lymphoid tissue (Fig. 6E). A key question is whether the local production of these autoantibodies is stimulated by cognate T-B interactions within the ectopic lymphoid tissue (consistent with a germinal center reaction) or by antigen-independent mechanisms, such as TLR signaling. Although unlike germinal centers, TMPD-induced ectopic lymphoid tissue did not contain FDC-M1$^+$ follicular dendritic cells (FDCs) (Fig. 1A), FDC-M1$^-$ FDCs have been described (34).

In humans, FDCs have been reported in lymphoid neogenesis arising in the stomach, rheumatoid synovium, salivary glands, and other locations (35-37), raising the possibility that the germinal center-like structures found in these sites are sites of cognate T-B interaction involved in autoantibody production. Conversely, autoantibodies can be produced extrafollicularly by B cells located at the border between the T cell zone and the red pulp of the spleen (22, 38, 39). This is a site where T cell-independent responses to foreign antigens occur and it has been shown that in AM14 rheumatoid factor transgenic mice, the activation of autoantibody production requires TLR signaling but not T cells (40).

The presence of AID and circle intermediates in TMPD-induced ectopic lymphoid tissue (Fig. 2) strongly suggests that B cell activation occurs locally. AID, an enzyme required for CSR and SHM (41, 42), is expressed in germinal centers (43). In addition, the presence of circle transcripts (Fig. 2C), transient intermediates of CSR, that at least *in vitro* disappear within 48 hours of being generated (14) strongly suggests that the ectopic lymphoid tissue is a site of CSR, arguing against the possibility that isotype switched B cells secondarily migrate there. However, although the presence of circle transcripts is suggestive of local

CSR, we cannot at present exclude the possibility that circle transcripts are degraded more slowly under *in vivo* conditions.

In addition, although characteristic of germinal center reactions, AID expression and CSR can be induced in B cells by TLR signaling (44-46). Thus, even though B cell activation occurs locally, since the U1 small ribonucleoprotein carries an endogenous TLR7 ligand (47), we cannot completely exclude the possibility that anti-Sm/RNP autoantibody production in the ectopic lymphoid tissue is antigen-independent and driven by TLR7 signaling, as has been reported for other autoantibodies. For instance, when injected with an IgG2a anti-chromatin antibody, AM14 transgenic mice deficient in T cell receptors generate AM14 (rheumatoid factor) antibody forming cells at frequencies comparable to those in TcR sufficient controls (40). The T cell independent activation of these autoantibody producing cells is mediated by dual engagement of the B cell receptor and Toll-like receptors. However, TLR signaling in TMPD-induced ectopic lymphoid tissue was insufficient to drive significant IgM or class-switched (IgG1, IgG2a) anti-Sm/RNP autoantibody production or SHM in TcR deficient mice (Fig. 6, Table 2), consistent with the possibility that cognate interactions between anti-Sm/RNP B and T cells take place in the ectopic lymphoid tissue, as also appears to be the case following immunization with exogenous antigens (24).

Examination of the immunoglobulin repertoires in individual lipogranulomas provides further evidence for the local activation of antigen-specific B cells within the ectopic lymphoid tissue. If B cells activated elsewhere secondarily populate the ectopic lymphoid tissue, different lipogranulomas might exhibit partially overlapping B cell repertoires, whereas if local expansion occurs (as suggested by B cell proliferation in the lipogranulomas, Fig. 1), the B cell repertoire should differ from lipogranuloma to lipogranuloma. In most cases, different B cell repertoires were found in the individual lipogranulomas from the same mouse. We did not identify immunoglobulin V_H-D-J_H sequences that were unequivocally shared by more than one lipogranuloma. In two cases (one from a TMPD treated mouse and one from a mineral oil treated mouse) identical V-D-J sequences were obtained from two different granulomas **(Figs.** 3-4**)**. However, due to the germline configuration of these sequences, it could not be determined whether they were derived from individual B cell clones or from two B cells that independently rearranged the same V-D-J. Similarly, the L-chain sequences from individual lipogranulomas did not overlap (data not shown). Strikingly, the B cell repertoire in individual lipogranulomas becomes highly oligoclonal following immunization with a foreign antigen (NP-KLH or NP-OVA) concomitant with the appearance of proliferating carrier-specific T cells in the same location (24). We conclude that autoantibody-secreting B cells most likely are activated locally within the ectopic lymphoid tissue. This activation may be dependent on cognate interactions with local antigen-specific T cells, although the possibility of T cell-independent, TLR-mediated B cell activation cannot be completely excluded. Further studies of the relative importance of T cells and TLR7 signaling for activating anti-Sm/RNP B cells in ectopic lymphoid tissue may help elucidate why ectopic lymphoid tissue is associated with a wide variety of humoral autoimmune disorders, including Hashimoto's thyroiditis (17), myasthenia gravis (48), multiple sclerosis (49), rheumatoid arthritis (28, 29), and Sjogren's syndrome (37, 50). Ectopic lymphoid tissue in TMPD lupus is a site of exuberant chronic Type I interferon production (9), which is required for the development of anti-Sm/RNP autoantibodies (51). The enrichment of anti-Sm/RNP B cells in the ectopic lymphoid tissue vs. spleen (Fig. 6E) highlights the potential importance of chronic inflammation in the pathogenesis of lupus autoantibodies, raising the possibility that ectopic lymphoid tissue formation (52, 53) or other forms of chronic inflammation (54) may be involved in the production of autoantibodies in human SLE as well in TMPD-lupus.

Acknowledgments

This work was supported by research grants R01-AR44731 and T32-007603 from the US Public Health Service and by generous gifts from Lupus Link, Inc. (Daytona Beach, FL) and Mr. Lewis M. Schott to the UF Center for Autoimmune Disease. Dr. Nacionales is the recipient of an Arthritis Foundation Postdoctoral Fellowship. The work was supported with resources and the use of facilities at the Malcolm Randall VA Medical Center, Gainesville, FL.

REFERENCES

1. Drayton DL, Liao S, Mounzer RH, Ruddle NH. Lymphoid organ development: from ontogeny to neogenesis. Nat Immunol. 2006; 7:344–353. [PubMed: 16550197]
2. von Andrian UH, Mempel TR. Homing and cellular traffic in lymph nodes. Nat Rev Immunol. 2003; 3:867–878. [PubMed: 14668803]
3. Cyster JG. Chemokines and cell migration in secondary lymphoid organs. Science. 1999; 286:2098–2102. [PubMed: 10617422]
4. Jacob J, Kassir R, Kelsoe G. In situ studies of the primary immune response to (4-hydroxy-3-nitrophenyl)acetyl. I. The architecture and dynamics of responding cell populations. J Exp Med. 1991; 173:1165–1175. [PubMed: 1902502]
5. McHeyzer-Williams LJ, McHeyzer-Williams MG. Antigen-specific memory B cell development. Annu Rev Immunol. 2005; 23:487–513. [PubMed: 15771579]
6. Jacob J, Kelsoe G. In situ studies of the primary immune response to (4-hydroxy-3-nitrophenyl)acetyl. II. A common clonal origin for periarteriolar lymphoid sheath-associated foci and germinal centers. J Exp Med. 1992; 176:679–687. [PubMed: 1512536]
7. Kratz A, Campos-Neto A, Hanson MS, Ruddle NH. Chronic inflammation caused by lymphotoxin is lymphoid neogenesis. J Exp Med. 1996; 183:1461–1472. [PubMed: 8666904]
8. Hjelmstrom P. Lymphoid neogenesis: de novo formation of lymphoid tissue in chronic inflammation through expression of homing chemokines. J Leukoc Biol. 2001; 69:331–339. [PubMed: 11261778]
9. Nacionales DC, Kelly KM, Lee PY, Zhuang H, Li Y, Weinstein JS, Sobel E, Kuroda Y, Akaogi J, Satoh M, Reeves WH. Type I interferon production by tertiary lymphoid tissue developing in response to 2,6,10,14-tetramethyl-pentadecane (pristane). Am J Pathol. 2006; 168:1227–1240. [PubMed: 16565497]
10. Satoh M, Kuroda Y, Yoshida H, Behney KM, Mizutani A, Akaogi J, Nacionales DC, Lorenson TD, Rosenbauer RJ, Reeves WH. Induction of lupus autoantibodies by adjuvants. J Autoimmun. 2003; 21:1–9. [PubMed: 12892730]
11. Potter M, MacCardle RC. Histology of developing plasma cell neoplasia induced by mineral oil in BALB/c mice. J Natl Cancer Inst. 1964; 33:497–515. [PubMed: 14207859]
12. Ulett GC, Ketheesan N, Hirst RG. Cytokine gene expression in innately susceptible BALB/c mice and relatively resistant C57BL/6 mice during infection with virulent Burkholderia pseudomallei. Infect Immun. 2000; 68:2034–2042. [PubMed: 10722599]
13. White HN. Restriction-PCR fingerprinting of the immunoglobulin VH repertoire: direct detection of an immune response and global analysis of B cell clonality. Eur J Immunol. 1998; 28:3268–3279. [PubMed: 9808196]
14. Kinoshita K, Harigai M, Fagarasan S, Muramatsu M, Honjo T. A hallmark of active class switch recombination: transcripts directed by I promoters on looped-out circular DNAs. Proc Natl Acad Sci U S A. 2001; 98:12620–12623. [PubMed: 11606740]
15. Satoh M, Weintraub JP, Yoshida H, Shaheen VM, Richards HB, Shaw M, Reeves WH. Fas and Fas ligand mutations inhibit autoantibody production in pristane-induced lupus. J Immunol. 2000; 165:1036–1043. [PubMed: 10878381]
16. Hamilton KJ, Satoh M, Swartz J, Richards HB, Reeves WH. Influence of microbial stimulation on hypergammaglobulinemia and autoantibody production in pristane-induced lupus. Clin Immunol Immunopathol. 1998; 86:271–279. [PubMed: 9557160]
17. Armengol MP, Juan M, Lucas-Martin A, Fernandez-Figueras MT, Jaraquemada D, Gallart T, Pujol-Borrell R. Thyroid autoimmune disease: demonstration of thyroid antigen-specific B cells

and recombination-activating gene expression in chemokine-containing active intrathyroidal germinal centers. Am J Pathol. 2001; 159:861–873. [PubMed: 11549579]

18. Arant SE, Griffin JA, Koopman WJ. VH gene expression is restricted in anti-IgG antibodies from MRL autoimmune mice. J Exp Med. 1986; 164:1284–1300. [PubMed: 3093628]
19. Barnes JL, Goni F, Heyermann H, Frangione B, Agnello V. Human rheumatoid factor cross-idiotypes. III. Bla monoclonal rheumatoid factor, prototype of the BLA cross-idiotype group, has distinct kappa chains related to the V kappa III subgroup and VH4 heavy chains. Arthritis Rheum. 1990; 33:1710–1715. [PubMed: 2122903]
20. Liu YJ, Johnson GD, Gordon J, MacLennan IC. Germinal centres in T-cell-dependent antibody responses. Immunol Today. 1992; 13:17–21. [PubMed: 1739427]
21. Wang D, Wells SM, Stall AM, Kabat EA. Reaction of germinal centers in the T-cell-independent response to the bacterial polysaccharide alpha(1-->6)dextran. Proc Natl Acad Sci U S A. 1994; 91:2502–2506. [PubMed: 7511812]
22. William J, Euler C, Christensen S, Shlomchik MJ. Evolution of autoantibody responses via somatic hypermutation outside of germinal centers. Science. 2002; 297:2066–2070. [PubMed: 12242446]
23. Mao C, Jiang L, Melo-Jorge M, Puthenveetil M, Zhang X, Carroll MC, Imanishi-Kari T. T cell-independent somatic hypermutation in murine B cells with an immature phenotype. Immunity. 2004; 20:133–144. [PubMed: 14975236]
24. Weinstein JS, Nacionales DC, Lee PY, Kelly-Scumpia KM, Yan XJ, Scumpia PO, Vale-Cruz DS, Sobel E, Satoh M, Chiorazzi N, Reeves WH. Colocalization of antigen-specific B and T cells within ectopic lymphoid tissue following immunization with exogenous antigen. J Immunol. 2008; 181:3259–3267. [PubMed: 18713997]
25. Aloisi F, Pujol-Borrell R. Lymphoid neogenesis in chronic inflammatory diseases. Nat Rev Immunol. 2006; 6:205–217. [PubMed: 16498451]
26. Cassese G, Lindenau S, de Boer B, Arce S, Hauser A, Riemekasten G, Berek C, Hiepe F, Krenn V, Radbruch A, Manz RA. Inflamed kidneys of NZB / W mice are a major site for the homeostasis of plasma cells. Eur J Immunol. 2001; 31:2726–2732. [PubMed: 11536171]
27. Hoyer BF, Moser K, Hauser AE, Peddinghaus A, Voigt C, Eilat D, Radbruch A, Hiepe F, Manz RA. Short-lived plasmablasts and long-lived plasma cells contribute to chronic humoral autoimmunity in NZB/W mice. J Exp Med. 2004; 199:1577–1584. [PubMed: 15173206]
28. Randen I, Mellbye OJ, Forre O, Natvig JB. The identification of germinal centres and follicular dendritic cell networks in rheumatoid synovial tissue. Scand J Immunol. 1995; 41:481–486. [PubMed: 7725067]
29. Schroder AE, Greiner A, Seyfert C, Berek C. Differentiation of B cells in the nonlymphoid tissue of the synovial membrane of patients with rheumatoid arthritis. Proc Natl Acad Sci U S A. 1996; 93:221–225. [PubMed: 8552609]
30. Bombardieri M, Barone F, Humby F, Kelly S, McGurk M, Morgan P, Challacombe S, De Vita S, Valesini G, Spencer J, Pitzalis C. Activation-induced cytidine deaminase expression in follicular dendritic cell networks and interfollicular large B cells supports functionality of ectopic lymphoid neogenesis in autoimmune sialoadenitis and MALT lymphoma in Sjogren's syndrome. J Immunol. 2007; 179:4929–4938. [PubMed: 17878393]
31. Satoh M, Reeves WH. Induction of lupus-associated autoantibodies in BALB/c mice by intraperitoneal injection of pristane. J Exp Med. 1994; 180:2341–2346. [PubMed: 7964507]
32. Satoh M, Kumar A, Kanwar YS, Reeves WH. Anti-nuclear antibody production and immune-complex glomerulonephritis in BALB/c mice treated with pristane. Proc Natl Acad Sci U S A. 1995; 92:10934–10938. [PubMed: 7479913]
33. Potter M, Wax JS, Blankenhorn E. BALB/c subline differences in susceptibility to plasmacytoma induction. Curr Top Microbiol Immunol. 1985; 122:234–241. [PubMed: 3930153]
34. Allen CD, Cyster JG. Follicular dendritic cell networks of primary follicles and germinal centers: phenotype and function. Semin Immunol. 2008; 20:14–25. [PubMed: 18261920]
35. Mazzucchelli L, Blaser A, Kappeler A, Scharli P, Laissue JA, Baggiolini M, Uguccioni M. BCA-1 is highly expressed in Helicobacter pylori-induced mucosa-associated lymphoid tissue and gastric lymphoma. J Clin Invest. 1999; 104:R49–54. [PubMed: 10562310]

36. Takemura S, Braun A, Crowson C, Kurtin PJ, Cofield RH, O'Fallon WM, Goronzy JJ, Weyand CM. Lymphoid neogenesis in rheumatoid synovitis. J Immunol. 2001; 167:1072–1080. [PubMed: 11441118]
37. Salomonsson S, Jonsson MV, Skarstein K, Brokstad KA, Hjelmstrom P, Wahren-Herlenius M, Jonsson R. Cellular basis of ectopic germinal center formation and autoantibody production in the target organ of patients with Sjogren's syndrome. Arthritis Rheum. 2003; 48:3187–3201. [PubMed: 14613282]
38. Shlomchik MJ. Sites and stages of autoreactive B cell activation and regulation. Immunity. 2008; 28:18–28. [PubMed: 18199415]
39. Jacobson BA, Panka DJ, Nguyen KA, Erikson J, Abbas AK, Marshak-Rothstein A. Anatomy of autoantibody production: dominant localization of antibody-producing cells to T cell zones in Fas-deficient mice. Immunity. 1995; 3:509–519. [PubMed: 7584141]
40. Herlands RA, Christensen SR, Sweet RA, Hershberg U, Shlomchik MJ. T Cell-Independent and Toll-like Receptor-Dependent Antigen-Driven Activation of Autoreactive B Cells. Immunity. 2008; 29:249–260. [PubMed: 18691914]
41. Muramatsu M, Kinoshita K, Fagarasan S, Yamada S, Shinkai Y, Honjo T. Class switch recombination and hypermutation require activation-induced cytidine deaminase (AID), a potential RNA editing enzyme. Cell. 2000; 102:553–563. [PubMed: 11007474]
42. Honjo T, Kinoshita K, Muramatsu M. Molecular mechanism of class switch recombination: linkage with somatic hypermutation. Annu Rev Immunol. 2002; 20:165–196. [PubMed: 11861601]
43. Muramatsu M, Sankaranand VS, Anant S, Sugai M, Kinoshita K, Davidson NO, Honjo T. Specific expression of activation-induced cytidine deaminase (AID), a novel member of the RNA-editing deaminase family in germinal center B cells. J Biol Chem. 1999; 274:18470–18476. [PubMed: 10373455]
44. He B, Qiao X, Cerutti A. CpG DNA induces IgG class switch DNA recombination by activating human B cells through an innate pathway that requires TLR9 and cooperates with IL-10. J Immunol. 2004; 173:4479–4491. [PubMed: 15383579]
45. Capolunghi F, Cascioli S, Giorda E, Rosado MM, Plebani A, Auriti C, Seganti G, Zuntini R, Ferrari S, Cagliuso M, Quinti I, Carsetti R. CpG drives human transitional B cells to terminal differentiation and production of natural antibodies. J Immunol. 2008; 180:800–808. [PubMed: 18178818]
46. Jegerlehner A, Maurer P, Bessa J, Hinton HJ, Kopf M, Bachmann MF. TLR9 signaling in B cells determines class switch recombination to IgG2a. J Immunol. 2007; 178:2415–2420. [PubMed: 17277148]
47. Kelly KM, Zhuang H, Nacionales DC, Scumpia PO, Lyons R, Akaogi J, Lee P, Williams B, Yamamoto M, Akira S, Satoh M, Reeves WH. "Endogenous adjuvant" activity of the RNA components of lupus autoantigens Sm/RNP and Ro 60. Arthritis Rheum. 2006; 54:1557–1567. [PubMed: 16645989]
48. Sims GP, Shiono H, Willcox N, Stott DI. Somatic hypermutation and selection of B cells in thymic germinal centers responding to acetylcholine receptor in myasthenia gravis. J Immunol. 2001; 167:1935–1944. [PubMed: 11489973]
49. Corcione A, Casazza S, Ferretti E, Giunti D, Zappia E, Pistorio A, Gambini C, Mancardi GL, Uccelli A, Pistoia V. Recapitulation of B cell differentiation in the central nervous system of patients with multiple sclerosis. Proc Natl Acad Sci U S A. 2004; 101:11064–11069. [PubMed: 15263096]
50. Stott DI, Hiepe F, Hummel M, Steinhauser G, Berek C. Antigen-driven clonal proliferation of B cells within the target tissue of an autoimmune disease. The salivary glands of patients with Sjogren's syndrome. J Clin Invest. 1998; 102:938–946. [PubMed: 9727062]
51. Nacionales DC, Kelly-Scumpia KM, Lee PY, Weinstein JS, Lyons R, Sobel E, Satoh M, Reeves WH. Deficiency of the type I interferon receptor protects mice from experimental lupus. Arthritis Rheum. 2007; 56:3770–3783. [PubMed: 17968932]

52. Massone C, Kodama K, Salmhofer W, Abe R, Shimizu H, Parodi A, Kerl H, Cerroni L. Lupus erythematosus panniculitis (lupus profundus): clinical, histopathological, and molecular analysis of nine cases. J Cutan Pathol. 2005; 32:396–404. [PubMed: 15953372]

53. Omokawa A, Wakui H, Okuyama S, Togashi M, Ohtani H, Komatsuda A, Ichinohasama R, Sawada K. Predominant tubulointerstitial nephritis in a patient with systemic lupus erythematosus: phenotype of infiltrating cells. Clin Nephrol. 2008; 69:436–444. [PubMed: 18538120]

54. Alarcon-Riquelme ME. Nucleic acid by-products and chronic inflammation. Nat Genet. 2006; 38:866–867. [PubMed: 16874327]

Reference List

1. Livak KJ, Schmittgen TD. Analysis of relative gene expression data using real-time quantitative PCR and the 2(−Delta Delta C(T)) Method. Methods. 2001; 25:402–408. [PubMed: 11846609]

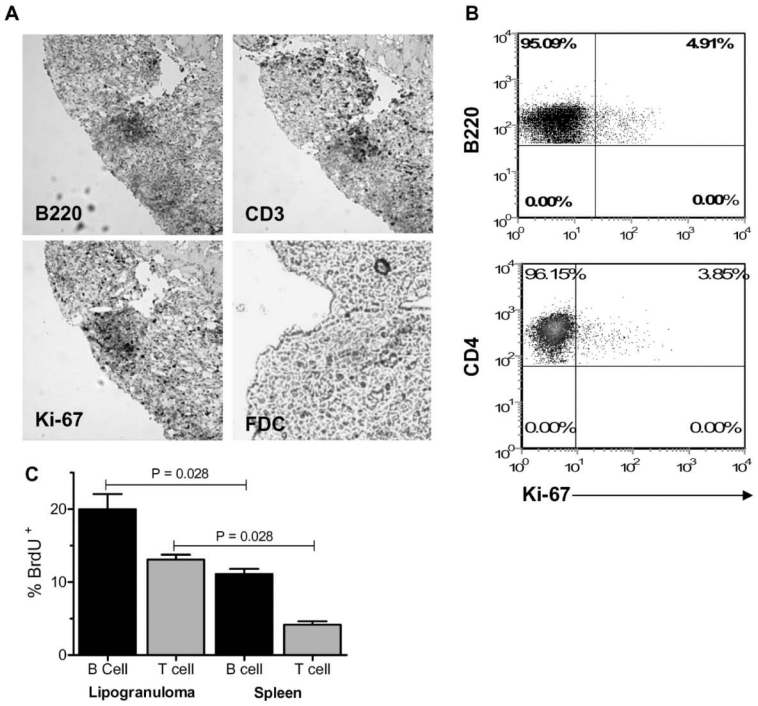

Figure 1. B and T cell proliferation in lipogranulomas

A, Immunohistochemistry of a TMPD-induced lipogranuloma (serial sections) demonstrating the presence of contiguous B cell ($B220^+$) and T cell ($CD3^+$) zones as well as cellular proliferation, as demonstrated by Ki-67 staining. Bottom right panel shows the absence of cells staining with the follicular dendritic cell marker FDC-M1 (FDC). **B,** Flow cytometry of lipogranuloma cells. Gates were set on either the B cells anti-CD45R (B220) or T cells (anti-CD4) and the percentage of cells staining with anti-Ki67 antibodies was determined. **C,** *In vivo* BrdU labeling of T and B cells in the lipogranulomas and spleens of TMPD-treated mice. Single cell suspensions were stained with anti-CD45R (B220), anti-CD3, and anti-BrdU antibodies. Data are expressed as the % of $BrdU^+$ B cells or T cells, respectively.

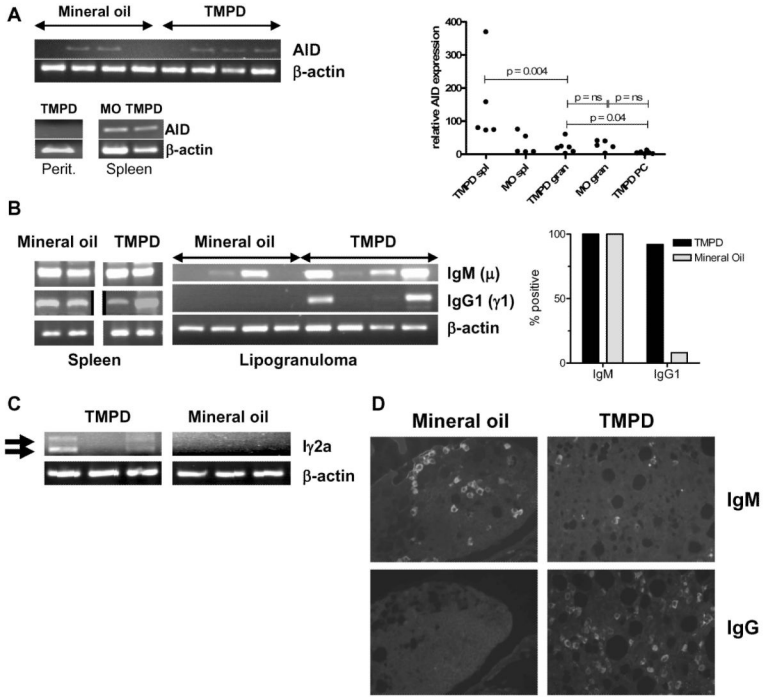

Figure 2. TMPD lipogranulomas contain class switched B cells

A, Lipogranulomas express AID. *Left*, cDNA from TMPD or mineral oil lipogranulomas, spleen, or peritoneal cells was amplified using primers specific for AID or β-actin and analyzed by agarose gel electrophoresis. *Right*, AID mRNA was quantified by real-time PCR normalized to 18S RNA. **B,** μ and γ H-chain transcripts. Lipogranuloma and spleen cDNA from mineral oil or TMPD treated mice was tested for expression of IgM and IgG1 by PCR using VHF1-8 and Cμ or Cγ1 reverse primers, respectively. *Left,* agarose gel of amplified PCR products from lipogranulomas or spleen. γ1 transcripts are seen strongly in two TMPD lipogranulomas (TMPD, lanes 1 and 4) and weakly in another (TMPD, lane 3). *Right,* frequencies of IgM and IgG1 production in TMPD vs. mineral oil lipogranulomas (4 individual lipogranulomas/mouse, 3 mice/group). ***C,*** Circle transcripts. Presence of isotype specific I promoter-Cγ2a transcripts in lipogranulomas from TMPD-treated but not in mineral oil treated mice. Circle transcripts were detected using Iγ2aF forward primer and CμR reverse primer. PCR product sizes closely approximated the expected sizes of 458 and 318 bp (14) (arrows). PCR using B-actin primers was used as a loading control. **D,** Direct immunofluorescence for IgM (top) and IgG (bottom) producing cells in lipogranulomas from mineral oil or TMPD-treated mice (green). Nuclei were visualized by DAPI staining (blue). Both IgM and IgG producing cells were detected in ectopic lymphoid tissue from TMPD-treated mice, but only IgM producing cells in tissue from mineral oil-treated mice.

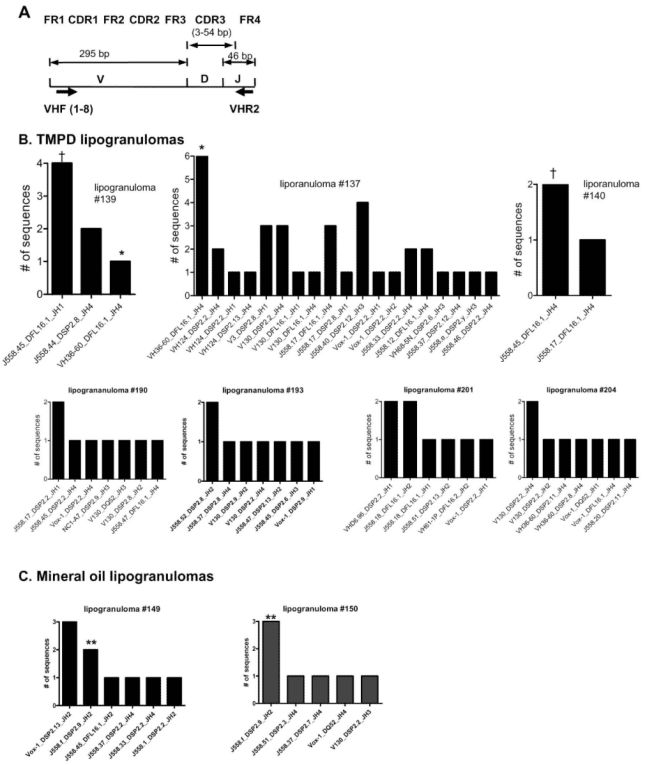

Figure 3. Individual TMPD-induced lipogranulomas contain distinctive populations of B cells

A, pooled forward primers (VHF1-8) and consensus reverse primer (VHR2) used for amplifying cDNA from lipogranulomas. **B,** H-chains recovered from lipogranulomas obtained from TMPD-treated BALB/c mice. Lipogranulomas #137, 139, and 140 were isolated from the same mouse. Lipogranulomas #190 and 193 were from a second mouse and lipogranulomas #201 and 204 from a third mouse. **C,** H-chains recovered from two lipogranulomas (#149 and 150) obtained from a mineral oil-treated BALB/c mouse.

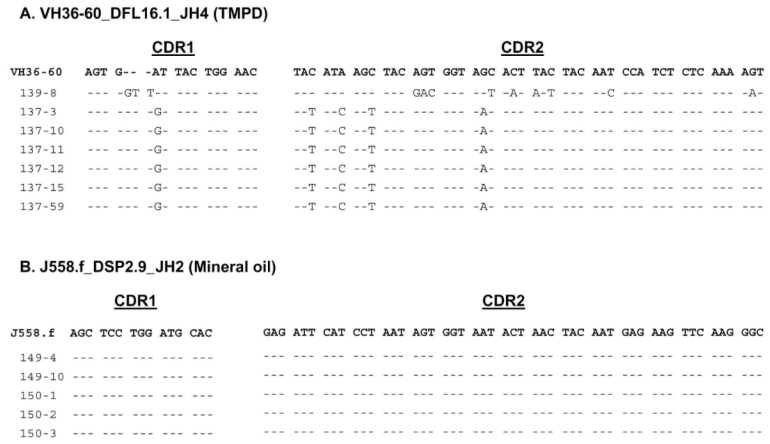

Figure 4. V_H sequences from TMPD-induced lipogranulomas

A, Sequence alignments of VH36-60-DFL16.1-JH4 H-chains isolated from lipogranulomas #137 and 139 (two individual lipogranulomas from a single TMPD-treated mouse). Sequences obtained from the two different granulomas were unrelated, whereas the 6 sequences in granuloma #137 were identical. **B,** Sequence alignments of J558.f-DSP2.9-JH2 H-chains isolated from two different lipogranulomas (#149 and 150) from a mineral oil-treated mouse.

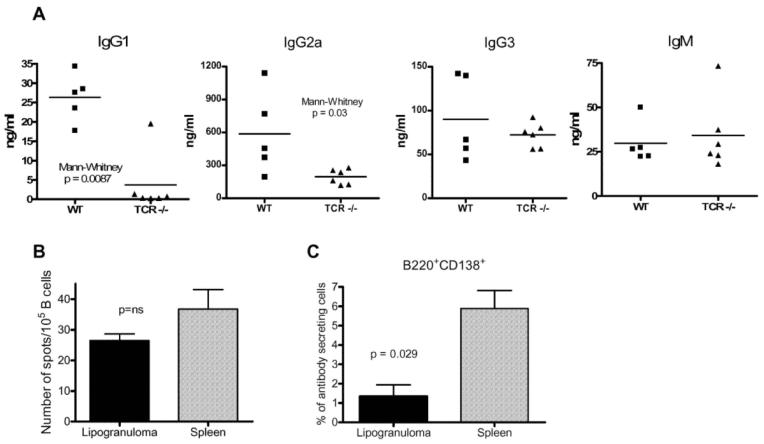

Figure 5. IgG1 and IgG2a induced hypergammaglobulinemia in TMPD-treated mice is T cell dependent

A, Serum samples were obtained from wild type C57BL/6J (WT, n = 5) or B6.129P2-*Tcrb*^{tm1Mom}*Tcrd*^{Tm1Mom} (n = 6) mice treated 3 months earlier with TMPD. IgG1, IgG2a, IgG3, and IgM levels were measured by ELISA and means were compared by the Mann-Whitney test. **B,** IgG production in lipogranulomas. Lipogranuloma cells and splenocytes from two mice were tested in quadruplicate for T cell dependent immunoglobulin secretion (IgG1+IgG2a+IgG2b) by ELISPOT assay. **C,** Quantification of plasmablasts in spleen and lipogranulomas. Pooled lipogranuloma and spleen cells from four TMPD-treated BALBc/J mice were stained with anti-B220 and anti-CD138 antibodies and analyzed by flow cytometry.

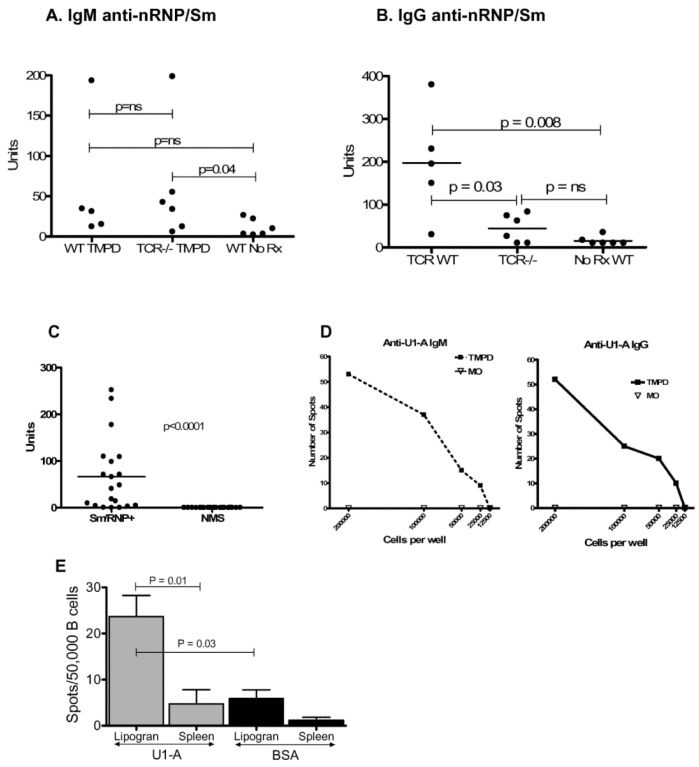

Figure 6. IgG anti-nRNP/Sm autoantibody production in TMPD-treated mice is T cell dependent

A and B, Serum samples were obtained from wild type C57BL/6J (WT, n = 5) or B6.129P2-*Tcrb*^{tm1Mom}*Tcrd*^{Tm1Mom} (n = 6) mice treated 3 months earlier with TMPD. IgM **(A)** and IgG **(B)** anti-nRNP/Sm antibody levels were measured by ELISA at a 1:500 serum dilution. Means were compared by the Mann-Whitney test. **C,** Reactivity of sera with recombinant U1-A protein (ELISA). Recombinant 6His-tagged U1-A protein was expressed in *E. coli* and purified on a Ni-NTA affinity column. Sera from 20 TMPD-treated BALB/c mice positive for anti-Sm/RNP autoantibodies and 20 normal BALB/c mouse sera were tested for reactivity with the recombinant antigen at a 1:100 dilution (ELISA). **D,** IgM and IgG ELISPOT assay with purified U1-A antigen using cells isolated from collagenase treated ectopic lymphoid tissue from an anti-RNP positive TMPD-treated mouse or an anti-RNP negative mouse treated with medicinal mineral oil. Representative of 3 experiments. **E,** IgG ELISPOT assay with purified U1-A or bovine serum albumin (BSA) antigens, using cells isolated from lipogranulomas (Lipogran) or spleens of anti-U1-A positive mice (n = 5). The frequencies of antigen-specific spots are expressed per 50,000 B cells. The frequency of anti-U1-A spots was higher in lipogranulomas than in spleen (P = 0.01, Mann-Whitney test) and the frequency of anti-U1-A spots was higher than the frequency of anti-BSA spots (P = 0.03, Mann-Whitney test).

TABLE I

Somatic hypermutation of H-chains from ectopic lymphoid tissue

				Number of mutations					
Treatment	**# of sequences**	**# of mice**	**# of lipogranulomas**	**FR R**	**FR S**	**CDR R**	**CDR S**	**R/S FR**	**R/S CDR**
TMPD	20	2	4	66	39	72	10	1.7	7.2
Mineral oil	20	2	4	23	11	16	2	2	8

FR, sequences from Framework 2 and 3

CDR, sequences from CDR 1 and 2

J Immunol. Author manuscript; available in PMC 2012 July 12.

TABLE II

Somatic hypermutation in ectopic lymphoid tissue from TcR deficient mice

			Framework		CDRs		R/S ratio	
Strain	# of lipogranulomas	# of sequences	R (%)	S (%)	R (%)	S (%)	FR	CDR
WT*	2	6	0.08	0.32	1.30	0.50	0.25	2.5
TcR KO	4	12	0	0	0.13	0	0	***

* WT, wild type; R = replacement mutations; S = silent mutations; FR, framework regions; CDR, complementarity determining regions

*** unable to calculate (zero denominator)

J Immunol. Author manuscript; available in PMC 2012 July 12.